Proceedings of 2014 Offshore Energy & Storage Symposium
Windsor, Onatrio, Canada
UWCAES Society
July 10-11, 2014

Evaluating the Underwater Compressed Air Energy Storage Potential in the Gulf of Maine

Carson Pete*, Jon G. McGowan†, and Walter Jaslanek‡
University of Massachusetts, Amherst, MA, 01003, USA

Abstract

The United States has recognized the need to offset current and future electrical demand with clean, renewable generation. However, plans for integration of high penetration levels of often variable and uncertain renewable energy, like offshore wind, pose significant challenges to utility gird operators and system planners. The intermittent nature of renewables can result in dramatic changes in system load, indicating a need for large-scale energy storage technologies that would allow renewables to be dispatched when needed. Among different storage technologies, pumped hydro storage, batteries and fuel cells have some inherent advantages over others but only compressed air energy storage (CAES) has the capacity of pumped hydro and potentially lowest overall capital and capacity costs. Advances in system compression designs and utilization of thermal energy storage has made CAES increasingly attractive, especially as new innovations in air storage technologies are now allowing CAES to break away from site specific geological formations like salt domes by allowing the air to be stored underwater in pressure vessels. In this paper, a thermodynamic evaluation of an idealized underwater pressure-balanced CAES system is conducted and compared to other large-scale underwater storage methods. Using the Gulf of Maine as a case study area, the thermodynamic relations are integrated in ArcGIS, a geospatial analysis program, to determine the energy storage resource potential for the New England area.

1. Introduction

In the last decade, there has been significant growth in land-based wind and solar power capacities in the United States. This growth is attributed to advancements in technology, demand to increase energy security, government subsidies, and other policy incentives driven by national and global environmental concerns and the demand to meet U.S. domestic energy goals from sustainable and renewable resources. In particular, offshore wind is estimated to make large contributions to future U.S. energy portfolios due to the offshore wind resource potential and accessibility near load centers [1]. With the focus on promoting high penetration levels of variable and uncertain renewable generation in the near future, the efficient and cost-effective integration of renewables has raised attention. One potential solution to this issue is to integrate energy storage technologies. Pumped Hydro Storage (PHS) and Compressed Air Energy Storage (CAES) are two cost effective, commercially proven utility-scale technologies suitable for providing extended durations of energy storage with flexible ramping capabilities and good part-load operations. Conventional PHS and CAES technologies are highly reliant on site specific geological formations to store the energy [2]. Furthermore, existing diabatic CAES systems expel heat from the compression process and are dependent on natural gas to reheat the air during the expansion process thus producing emissions and having low to moderate overall efficiencies of 25-45%. Second and third-generation approaches to system design like adiabatic CAES (A-CAES) coupled with Thermal Energy Storage (TES) have the potential to improve cycle performance efficiencies up to 70-80% and eliminate emissions altogether [3]. Furthermore, new underwater air storage methods and technologies are breaking the dependence of site specific geological formations giving it a promising future for potential applications near coastal load centers and mitigating forthcoming offshore wind power issues. Several companies and university groups are currently investigating new compression and energy storage techniques that have the potential for grid-scale renewable integration and offshore applications. SustainX is developing the world's first grid-scale, near isothermal CAES that utilizes a foam-based heat exchange process[1]. HydroStor, a Toronto based company, plans to build a 1MW A-CAES demonstration plant with 4MWh of underwater storage capacity 5km off the shore of Lake Ontario at a depth of 80m this year.[2] Additionally, the Precision Engineering Research Group at MIT is developing prototypes of an underwater PHS vessel that would additionally act as an anchor for deep-water floating offshore wind turbines.[3] Given this recent development and interest of supporting renewable energy integration, in this paper we evaluate and compare three idealized CAES systems that are coupled to an underwater, constant-pressure air storage system. Furthermore, we compare the

[1] www.sustainx.com
[2] See Worlds first UW-CAES facility: www.hydrostor.ca/project
[3] http://pergatory.mit.edu/ores/

*PhD Candidate in Mechanical Engineering, corresponding author, cpete@ecs.umass.edu
†Professor of Mechanical Engineering
‡PhD Candidate in Ecology and Conservation

CAES results to an idealized underwater PHS system. The results from the analysis are then integrated into Esri's ArcGIS program to determine the underwater energy storage potential using the Gulf of Maine as a case study. The methodology, results, and implications are discussed.

2. Thermodynamics of Idealized Cases

To understand the characteristics and storage potential of the charging and discharging process of an idealized, constant-pressure, Underwater CAES (UW-CAES) storage system, the configuration shown in Fig. 1 will be analyzed. Three separate compression models will be considered and the energy storage densities will be compared. An ideal adiabatic model is considered assuming all the heat generated from the compression phase is taken out of the system via an ideal TES system and later, added back into the system prior to expansion without losses. To find the lower limit of energy storage density of the adiabatic model, a second model will assume no TES. This can be thought of reducing the efficiency of the TES down to zero and essentially letting the system store the hot, less dense air. For these models, it is assumed that the charge and discharge processes are adiabatic and the compressor and turbine are reversible. Last, an isothermal model will assume the air is compressed at constant temperature in a reversible manner. During the charging process, atmospheric air is compressed to the storage pressure, which remains at constant pressure by allowing storage volume change. The discharge process through the turbine is reversible; however in the case of no TES, the mixing of cold exhaust with the atmosphere is irreversible.

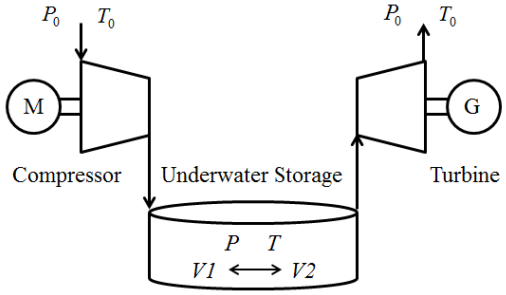

Figure 1. Configuration of ideal constant-pressure, CAES case with no thermal storage.

According to the first law of thermodynamics the general open system energy rate balance is [4]:

$$\dot{Q}_{Net,\mathrm{In}} - \dot{W}_{Shaft,\mathrm{NetOut}} = \frac{d}{dt}\int_{CV} e\rho dV + \sum_{OUT} \dot{\mathrm{m}}\left(\frac{P}{\rho}+e\right) - \sum_{IN} \dot{\mathrm{m}}\left(\frac{P}{\rho}+e\right) \tag{1}$$

Where $\dot{Q}$ and $\dot{W}$ are the net heat and work transport rate terms, $\dot{m}$ is the mass flow rate across an inlet or outlet and e the total energy per unit mass for the control volume and flow streams. Additionally, it is assumed that air behaves as an ideal gas with constant specific heats.

2.1 The Charging Process No-TES Model

Using a control volume around the compressor (reversible) neglecting potential and kinetic energy terms yields:

$$\dot{W}_C = \mathrm{h}_{Out}\dot{\mathrm{m}}_{Out} - \mathrm{h}_{In}\dot{\mathrm{m}}_{In} = C_P\,\mathrm{T}_0\left[\left(\frac{P}{P_0}\right)^{\frac{\gamma-1}{\gamma}} - 1\right]dm \tag{2}$$

γ is defined as the ratio of specific heats (C_P/C_V) and h is the specific enthalpy of the fluid. The differential mass (dm) entering the storage vessel is unknown; but using Equation (1) with a control volume around the storage vessel gives:

$$\mathrm{dm}_{In} = \frac{P}{RT_{Exit}}dV = \frac{P_0}{RT_0}\frac{P^{\frac{1}{\gamma}}}{P_0}\,dV \tag{3}$$

Substituting Equation (3) into (2) and integrating over volume change ΔV, yields:

$$W_C = C_P\,\mathrm{T}_0\left(\left(\frac{P}{P_0}\right)^{\frac{\gamma-1}{\gamma}} - 1\right)\left(\frac{P_0}{RT_0}\left(\frac{P}{P_0}\right)^{\frac{1}{\gamma}}\Delta V\right) \tag{4}$$

Thus, the non-dimensional work becomes:

$$\frac{W_C}{P_0 \Delta V} = \frac{\gamma}{\gamma - 1}\left(\frac{P}{P_0} - \left(\frac{P}{P_0}\right)^{1/\gamma}\right) = \frac{\gamma}{\gamma - 1}\left(\beta - (\beta)^{1/\gamma}\right) \tag{5}$$

Given β is the pressure ratio. Substituting Equation (5) into (1) and noting that $Q = 0$ for the system, we see that the compressor work is equal to the total energy stored in the system. It is also noted that the compressor work is independent of T and that the storage temperature is invariable during the compressing process. This can be verified using Equation (3) which combined with the equation of state of an ideal gas shows:

$$\frac{dm}{m} = \frac{dV}{V} \rightarrow T_{Initial} = T_{Final} \tag{6}$$

2.2 The Discharging Process No-TES Model

During the discharge process, the compressed air from the storage vessel will undergo a reversible adiabatic expansion through the turbine, generating electricity. However, because the subsequent mixing of the cold exhaust with the atmosphere is irreversible, a fictitious heater is required to represent the mixing. The exiting temperature of the turbine is given by:

$$T_{Exit} = T\frac{1}{\beta}(\beta)^{\frac{1}{\gamma}} \tag{7}$$

A control volume analysis is conducted around the heater and turbine. Substituting ideal gas relations and the equations for the differential mass and heat input, the non-dimensional work of the integral over the total volume change is found to be:

$$\frac{W_T}{P_0 \Delta V} = \frac{\gamma}{\gamma - 1}\left((\beta)^{1/\gamma} - \beta\right) \tag{8}$$

Thus, the turbine and compressor work are found to be equal despite having irreversibilities present in the discharge process.

2.3 The Adiabatic Model

To simulate an idealized A-CAES process, Fig. 2 is now analyzed. In addition to the assumptions made from the prior analysis in section 2.1, it is assumed that all of the heat generated from the compressor is captured and stored in a reversible process and then released back into the system prior to expansion through the turbine.

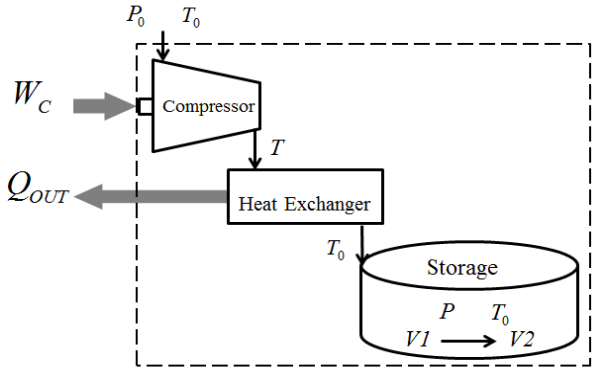

Figure 2. Configuration of the charging process of an ideal constant-pressure, adiabatic UW-CAES system.

A control volume analysis shows the non-dimensional work input for the charging process is:

$$\frac{W_C}{P_0 \Delta V} = \frac{\gamma}{\gamma - 1}\beta\left(1 - (\beta)^{\gamma - 1/\gamma}\right) \tag{9}$$

Furthermore, subsequent substitution of these relations back into Equation (1) shows the compressor work is equal to the internal energy change of the system. Analyzing the discharge process we find the turbine work is equal to the compressor work.

2.4 Isothermal Model

The model derived in the section 2.1 can also be converted to analyze an idealized isothermal compression system with the constant pressure and temperature by simply allowing the exiting temperature of the compressor to equal

the ambient temperature. Using a control volume around the compressor and storage vessel yields the following equation for the non-dimensional work:

$$\frac{W_{Iso}}{P_0 \Delta V} = \beta \ln(\beta) \tag{10}$$

With no heat input into the system, it can be shown that the isothermal work is equal to the stored energy of the system.

3. Energy Density Comparison

The energy storage densities for the ideal, underwater CAES models are both a function of hydrostatic pressure for a given water depth and the storage volume. To investigate and compare energy densities, the water depth z of the adiabatic model is solved for given the following parameters: $\rho_{H2O} = 1000 kg/m^3$, $g = 9.81 m/s^2$, $\gamma_{air} = 1.4$, $P_0 = 1atm = 101,325Pa$, the absolute pressure is given by $P_{abs} = P_0 + \rho g h$ and an energy density $\Delta U / \Delta V$ of $1kWh/m^3$

$$\frac{\Delta U}{P_0 \Delta V}_{Adiabatic} = \frac{\gamma}{\gamma - 1} \frac{P_{abs.}}{P_0} \left(\left(\frac{P_{abs}}{P_0} \right)^{\gamma - 1/\gamma} - 1 \right) \tag{11}$$

$$Z = 99m \rightarrow P = 1.07MPa \rightarrow \frac{1kwh}{m^3}$$

Thus to produce $1kWh/m^3$ a depth of 99m is required. Given these same parameters, the Non-Adiabatic model requires a depth of 176m to produce the same storage density while the isothermal model results in a depth of 130m required. In the case of underwater PHS, the storage potential relies on high pressure heads to generate sufficient amounts of electricity. To compare the underwater CAES energy density to an equivalent PHS system, the following storage capacity equation is given by [5]:

$$S_{PSH} = V \rho g H n \tag{12}$$

Where V is the volume of water that is passed through the system given in m^3, ρ is the density of water in kg/m^3, g is the acceleration due to gravity in m/s^2, H the effective head in m, and n the efficiency. Assuming an ideal system with $n = 100\%$, the PHS energy density (S_{PHS}/V) given equivalent parameters and head equal to the depth found from Equation (11), the PHS storage density is found to be $0.30kWh/m^3$, equivalently, in order to generate $1kWh/m^3$ a depth of 367 m is required. Fig. 3 below illustrates the energy densities of the CAES and PHS models as a function of water depth.

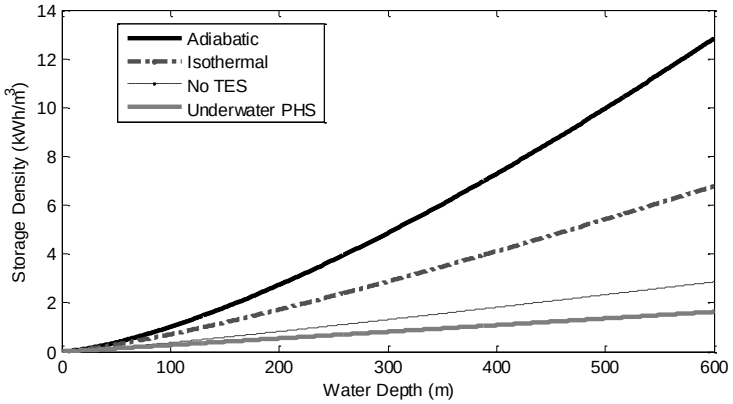

Figure 3: Energy storage densities of idealized underwater PHS and CAES models given water depth.

As shown, the adiabatic model has the highest storage density followed by the isothermal model. Surprisingly, the non-adiabatic model actually shows a higher energy storage density then the underwater PHS model.

4. Underwater Storage Potential

In order to illustrate the underwater storage potential using the idealized adiabatic model, the Gulf of Maine (GoM) is used as a case study. The GoM is a unique marine environment located off the shores of southeastern Canada and Coastal New England. The gulf encompasses over 170,000 square kilometers of ocean and has an average depth of 150m [6]. The shores of the GoM are bounded by New Brunswick, Nova Scotia, Maine, New Hampshire and

Massachusetts. Cape Cod and Cape Cod Bay define the southern boundaries while Georges Bank defines its most southwestern boundary. Additionally, the GoM exhibits an excellent offshore wind resource. In particular, the coast of Maine has one of the best offshore wind resources in the U.S., with 156 GW of capacity within approximately 90km and 80% of this capacity resides in waters deeper than 60m [7]. Furthermore, as recommended by the Maine Ocean Energy Task Force, supported by the Maine Legislature, Maine has constructed an initiative to build a network of five gigawatts of floating offshore wind farms, 35-90 km offshore by 2030 [8].

For this study, we concentrated on U.S. Waters within the GoM. Our study area is defined by the coastlines of Maine, New Hampshire, and eastern Massachusetts. The southern boundary is defined by the Cape Cod bay region and the eastern boundary is defined by the U.S. exclusive economic zone boundary. The entire study area covers 75,775 square kilometers. Existing source bathymetry raster data was collected from NOAA's National Geophysical Data Center where the data was created using NOAA's Costal Relief Model at 3 arc-second (approximately 90m) resolution.[4] Base map data was collected from the Northeast Ocean Data Center.[5] All data layers were integrated into ESRI ArcGIS Geographic Information Systems (GIS) software.[6] Using the Spatial Analysis extension in ArcGIS, Map Algebra was performed to calculate a new storage density value for each cell in the grid from the energy density Equation (11). The resulting raster dataset was then reclassified into a new raster dataset with each class defined in 50m depth increments and 50km increments of distances from the coastline. To determine the distances from shore, a GIS polygon layer was created from a coastline polyline file that was buffered in increments of 50km. The results from this analysis are shown below in Fig. 4.

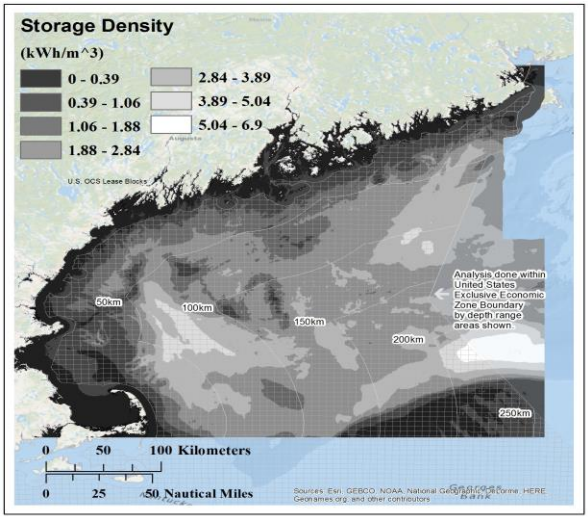

Figure 4. Idealized UW-CAES storage density map for the New England area in the Gulf of Maine.

As shown, the storage densities are distributed into seven storage density classes corresponding to 50m increments in depth (e.g. 0-50m has an equivalent storage density of 0-0.39) , with the exception of the last class depicted by the white color band, which has a corresponding depth range of 300m to 375m. This is due to the fact that only a small section of the total study area corresponds to these depths and lies in the distance region five zone. As a reference overlay, the Bureau of Ocean and Energy Management's (BOEM) Outer Continental Shelf lease blocks are shown by the white grid and are approximately 4.8km by 4.8km. For each distance region, the storage density values were aggregated to determine a total area for each storage class type. The capacity of storage, given in terawatt-hours, was determined by analyzing the distributions of storage densities for each region and within each class to find the mean value. The results are summarized below in Table 1. For our study area, the storage capacity generally peaks at a depth class of four (e.g. 150-200m) for each region. Region two has the highest storage area potential of 9,617 square kilometers at a class 4 depth and corresponds to just over 23 TWh of underwater storage capacity. The near shore resources of region one exhibits several areas along the Maine Coast line with storage density classes four or better, and one area near the Boston region shows a class 6 resource. Cumulatively, the New England area of the

[4] http://www.ngdc.noaa.gov/
[5] http://www.northeastoceandata.org/
[6] All data was converted to NAD 1983 UTM Zone 19M coordinate system.

GoM has over 110 TWh of potential underwater storage of class four or better resources. To put this into energy into context, this is equivalent of running the entire U.S. electrical load for ten days straight.[7]

Table 1. Cumulative underwater storage resource potential for Gulf of Maine.

Region	(1) 0-50km		(2) 50-100km		(3) 100-150km		(4) 150-200km		(5) 200-250km		TOTAL	
Class	Area m^2	Capacity TWh	Area m^2	Capacity TWh	Area m^2	Capacity TWh	Area m^2	Capacity TWh	Area m^2	Capacity TWh	Area m^2	Capacity TWh
1	11190	**2.1**	89	**0.016**	238	**0.044**	1445	**0.26**	941	**0.17**	13904	**2.5**
2	9145	**6.2**	378	**0.27**	476	**0.32**	426	**0.29**	1495	**1.0**	11919	**8.1**
3	5793	**8.6**	3006	**4.5**	829	**1.2**	130	**0.19**	70	**0.11**	9828	**15**
4	3222	**7.7**	9617	**23**	8124	**19**	3775	**9.1**	214	**0.51**	24952	**60**
5	1595	**5.2**	5517	**18**	3665	**12**	1966	**6.4**	373	**1.2**	13116	**43**
6	83	**0.35**	1037	**4.4**	170	**0.72**	14	**0.061**	542	**2.3**	1847	**7.8**
7	0	**0**	0	**0**	0	**0**	0	**0**	211	**1.1**	211	**1.1**

5. Conclusions

The increasing role of variable renewable energy resources, like offshore wind, in the grid has prompted concerns about grid reliability and raised concerns of how much of these resources can contribute before enabling technologies such as CAES are needed. In this study we analyzed and compared three ideal CAES models coupled with a constant pressure underwater storage system to an ideal underwater PHS system. The comparisons show that the adiabatic, UW-CAES has the highest storage density and requires the least water depth to effectively store the compressed air. The underwater PHS had the least storage density. The equation describing the internal energy stored in the adiabatic system was then integrated into ArcGIS to create a resource map for the New England region in the Gulf of Maine. Results show that a vast potential storage resource is available, most of which resides in waters less than 100km from the coastline and near major load centers, like the Boston area, in water depths that approach 200m.

6. Future Work

This initial study is part of a larger study being conducted to determine the theoretical applications and value of utilizing offshore CAES systems to mitigate the variability and uncertainty associated with planned, large-scale offshore wind energy development in the New England region. Only by comparing CAES models and storage systems will an optimized system be visualized. A build out of an offshore CAES plant will be conducted where simulated offshore wind power and loads from the NE-ISO will be utilized to determine the potential economic and operational value to both the grid system and the wind farm. Additionally, the integration of GIS software will enable a suitability analysis of the CAES system and will help address the environmental implications of storing compressed air on the ocean floor.

7. Acknowledgements

This work is supported by the NSF-sponsored IGERT: Offshore Wind Energy Engineering, Environmental Science, and Policy (NSF DGE-1068864).

8. References

[1] W. Musial, B. Ram, Large-Scale Offshore Wind Power in the United States: Assessment of Opportunities and Barriers, NREL TP-500-40745, (2010) 1-2.
[2] S. Sundararagavan, E.Baker, Evaluating Energy Storage Technologies for Wind Power Integration, Elsevier, Solar Energy 86, (2012) 2707-2717.
[3] B. Elmegaard, B. Wiebke, Efficiency of Compressed Air Energy Storage, Proceedings of 24th International Conference on Efficiency, Cost, Optimization, Simulation and Environmental Impact of Energy Systems,2011.
[4] Y. Cengel, M. Boles, Thermodynamics: An Engineering Approach, McGraw Hill Ed., New York, 2011, p.250.
[5] W. Tong, Wind Power Generation and Wind Turbine Design, WITPress, Boston, 2010, p.666.
[6] N. Wolff, L. Incze, Hypsometric Characterization of the Gulf of Maine, Georges Bank, Scotian Shelf and Neighboring Continental Slope, Census of Marine Life, http://www.gulfofmaine-census.org/about-the-gulf/physical-characteristics/bathymetry/hypsometric-characterization-of-the-gulf-of-maine-georges-bank-scotian-shelf/, Accessed May 2014.
[7] M. Schwartz, D. Heimiller, D. Haymes, W. Musial, Assessment of Offshore Wind Resources for the United States. NREL TP-500-45889, (2010) 16.
[8] UMaine, James W. Sewall Company, Maine Deepwater Offshore Wind Report, University of Maine, (2012) 25.

[7] Based off of U.S. 2013 load and generation data from U.S. Energy Information Administration website: http://www.eia.gov/electricity/